J. Phys. B: At. Mol. Opt. Phys. 27 (1994) 2511–2520. Printed in the UK

Excitation and ionization of H(2s) by proton impact

Z Chen†, B D Esry‡, C D Lin† and R D Piacentini§

† Department of Physics, Kansas State University, Manhattan, KS 66506, USA

‡ Department of Physics, University of Colorado, Boulder, CO 80309, USA

§ Instituto de Fisica de Rosario (CONICET) and Departamento Fisica, Facultad de Ciencias Exactas, Ingenieria Argrimensura, Universidad Nacional de Rosario, Av. Pellegrini 250, 2000 Rosario, Argentina

Received 10 January 1994, in final form 8 March 1994

Abstract. The two-centre atomic orbital close-coupling expansion method is used to study the excitation and ionization processes in collisions of protons with metastable hydrogen H(2s). The excitation cross sections to $n = 3$ and 4 and the averaged dipole moments are compared with the eikonal impulse distorted wave approximation calculations by Rodriguez and Miraglia and the one-centre expansion calculation by Ford *et al*. General agreement is found at high impact energies, but the difference in dipole moments between the present calculation and the EIA calculation at low energies is very large. We also examine the propensity rule for the magnetic substate distributions in the excitation cross sections in the 'natural' frame of reference.

1. Introduction

Collision processes involving the metastable hydrogenic H(2s) state occur in astrophysical and laboratory plasmas. Experimental data for the excitation, charge transfer and ionization cross sections by protons and other charged particles are not available. Thus, most of the collisional data involving H(2s) targets have been obtained by theoretical calculations (Blanco *et al* 1986, 1987, Schultz *et al* 1991, Esry *et al* 1993, Rodriguez and Miraglia 1994, Ford *et al* 1994). In order to examine the accuracy and the validity of these theoretical results, it is desirable to compare these results to those obtained from different theoretical models.

In this article we employed the two-centre atomic orbital expansion method to calculate the excitation and ionization cross sections for protons colliding with H(2s) in the 5–80 keV region. This particular close-coupling method has been successfully applied to collisions with target atoms in the ground state (Fritsch and Lin 1991), and in recent years also has been applied to collisions with target atoms in excited states. In the latter, the calculations (Dubois *et al* 1993) are mainly used to compare with experiments involving Na atoms in excited states (Dowek *et al* 1990, Campbell *et al* 1990, Richter *et al* 1993).

In carrying out close-coupling calculations involving target atoms in excited states, the major difficulty is to ensure that the results have converged. At collision energies where the projectile ion speed is faster than the orbital speed of the target electron, the collision processes populate a large number of final states. In a close-coupling calculation, these final states have to be included in the basis set, and the size of the numerical calculation can become too large to be practical. For the present collision system, we include all the dominant channels in the energy region considered. The results can be used to compare with two other recent calculations—one based on the eikonal impulse distorted

0953-4075/94/122511+10$19.50

wave approximation (EIA) (Rodriguez and Miraglia 1994) which is expected to be valid at higher collision energies, and another which is based on a one-centre close-coupling calculation (Ford *et al* 1994). The latter employed basis functions only on the target centre, and a very large basis set was used.

The theoretical method and the basis functions included in the calculation are briefly described in section 2. The results for the excitation cross sections to $n = 3$ and $n = 4$ and the total ionization cross sections are presented in section 3. They are also compared to the EIA results of Rodriguez and Miraglia (1994) and the results of Ford *et al* (1994). We also investigated two other quantities: the orientation of the excited states and the dipole moments for the $H(n = 3)$ manifold. We examined the orientation, or more precisely, the magnetic substate distributions for the 3p and 3d states that are populated by the excitation process. Using these distributions, we checked the validity of the propensity rule derived previously from collisions with ground state atoms (Andersen and Nielsen 1987, Lin *et al* 1989). We calculated the integrated dipole moments for the $H(n = 3)$ manifold to examine whether they are consistent with the results obtained from earlier works. We conclude this paper with a short summary in section 4. Atomic units are used throughout this work.

2. Theoretical methods

The two-centre atomic orbital close-coupling expansion method has been widely used to study ion–atom collisions at intermediate and low collision energies (Fritsch and Lin 1991). In this work, the trajectory of the projectile is taken to be a straight line. The time-dependent Schrödinger equation is then solved at each fixed impact parameter b. The transition cross section is obtained by integrating the square of the modulus of the corresponding transition amplitudes over the impact parameter plane. Slater-type orbitals are used on both centres to construct a set of atomic orbitals. The resulting set of atomic states consists of true hydrogenic ground and excited states, as well as a number of pseudostates which approximate the continuum states of the atomic hydrogen.

Since the initial state is H(2s), which is easily excited, ionized or captured to the projectile, a large number of basis functions were used in this calculation. We included 68 traveling atomic states on each collision centre consisting of the exact hydrogenic bound states for n up to 5, plus some pseudostates with negative and positive energies. It was necessary to include relatively high angular momentum states—$l = 0$–4—as they are very important for achieving convergence of the partial cross sections. To test the convergence of our calculation, we increase the number of states until each individual probability remains the same within 1 to 2%. As usual, it was easier to achieve convergence for the total cross section than for the partial cross section to each individual state. Furthermore, it was easier to achieve convergence for the excitation processes than for the ionization processes, presumably because for the latter the electron is not localized in configuration space and is not easily represented by a finite number of pseudostates. Our calculated ionization cross sections include contributions from both the total excitation and charge transfer cross sections to the positive energy pseudostates, i.e., we included direct ionization and capture to the continuum processes. We did not perform the projection to the real continuum states as done by Shakeshaft (1978) which is important when much higher precision is desired. Capture and excitation to negative pseudostates are very small.

Table 1. Cross sections (in 10^{-16} cm^2) of total electron capture, σ_c, excitation to $n = 3$ and $n = 4$, $\sigma_e(3)$ and $\sigma_e(4)$, and ionization, σ_i.

E (keV)	σ_c	$\sigma_e(3)$	$\sigma_e(4)$	σ_i
4	55.28	10.70	3.24	4.86
16	5.49	21.43	4.82	18.10
25	2.08	21.04	4.93	16.57
36	0.83	17.04	4.15	15.75
50	0.38	15.04	2.91	11.01
80	0.12	13.13	2.49	7.94

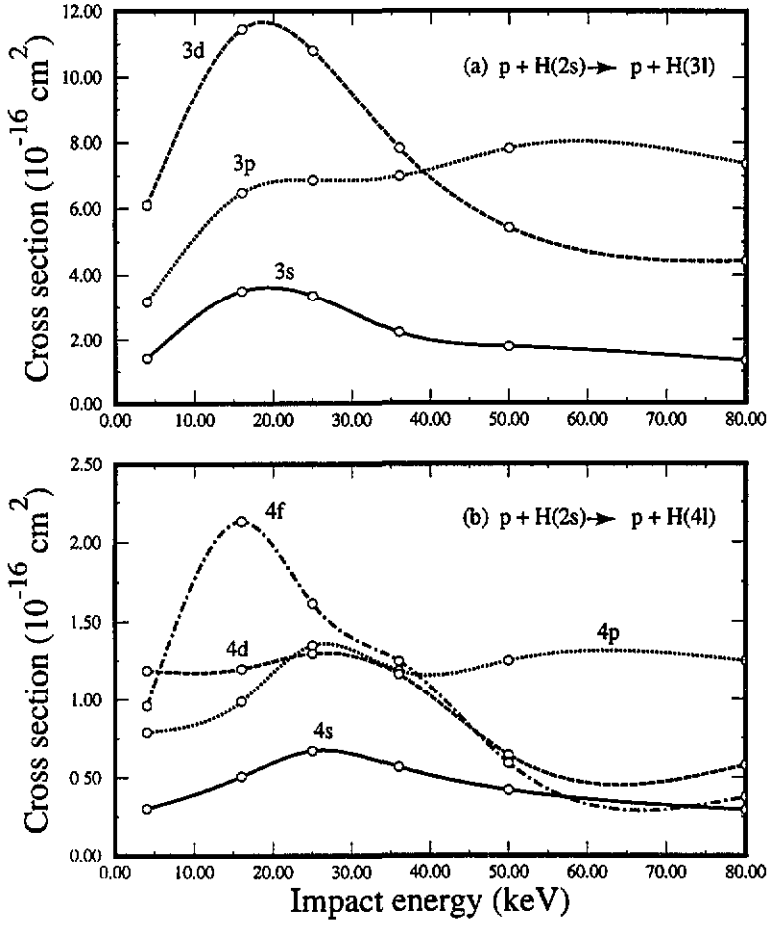

Figure 1. The close-coupling calculation of the total excitation cross sections in p + H(2s). (*a*) Excitation to $3l$; (*b*) excitation to $4l$.

3. Results and discussion

3.1. Excitation cross sections

In table 1, we list the cross sections of total electron capture, excitation and ionization. In the collision energy range above 15 keV, the dominant transition channels for p + H(2s) collisions are excitation to $n = 3$ states and ionization. The electron capture cross section at

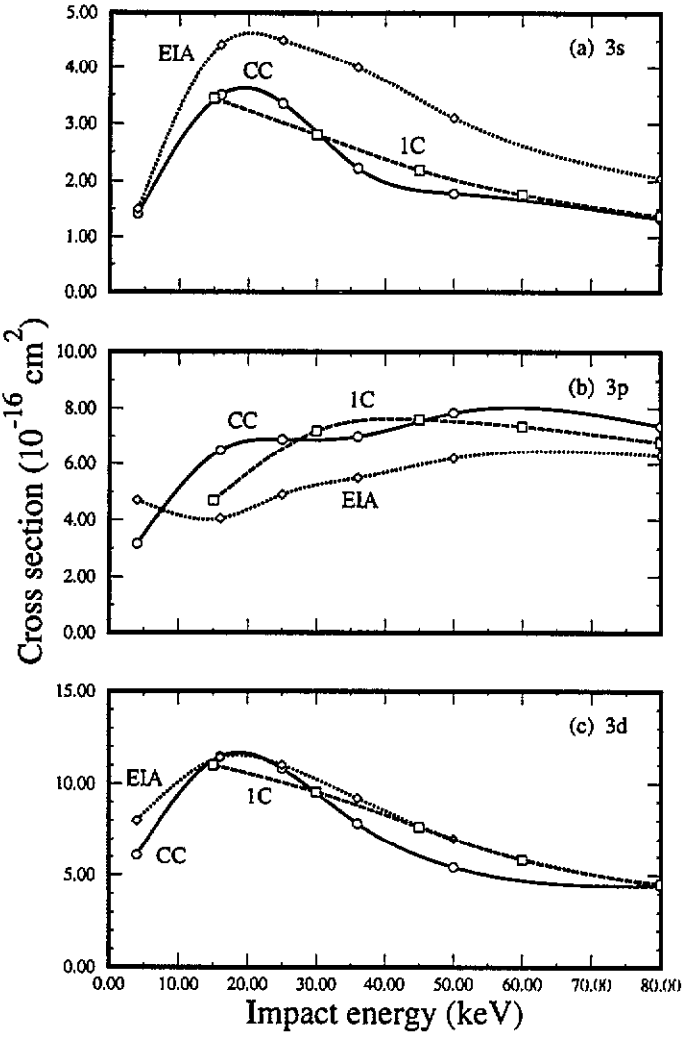

Figure 2. Total excitation cross sections to (*a*) 3s, (*b*) 3p and (*c*) 3d in p+H(2s) collisions from various calculations. Full curves, the present close-coupling calculation (CC); dotted curves, the eikonal impulse distorted wave approximation (EIA) calculation; broken curves, the one-centre expansion (1C).

these energies is at least one order of magnitude smaller. Excitation cross sections to $n = 4$ are about five times smaller than to $n = 3$ over the energy range considered. In figure 1, we plot the total excitation cross sections from H(2s) to $3l$ and $4l$ states. The circles indicate the energy points calculated. We notice that the excitation cross sections to the s states is always the smallest. At lower collision energies, where the interaction time is relatively long, excitations to 3d and 4f states are the dominant ones in the respective $n = 3$ and 4 manifolds. These states have the highest angular momentum possible in that manifold. This indicates that large angular momentum transfers in excitation processes are preferred at low collision energies. At higher collision energies, 3p and 4p are the dominantly excited states; these states are populated by direct dipole allowed transitions from the initial 2s state.

To compare with other calculations, we show in figure 2 the excitation cross sections

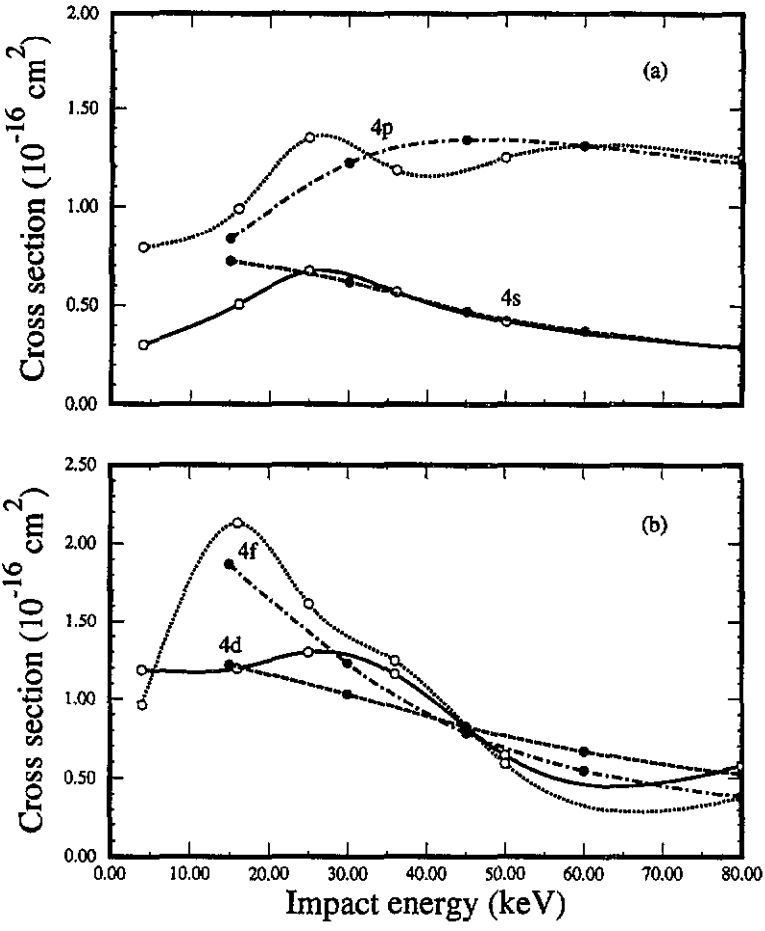

Figure 3. Total excitation cross sections to (*a*) 4s and 4p, and (*b*) to 4d and 4f. Curves with open circles are for the close coupling calculation and the curves with full circles are the one-centre expansion calculation.

to $n = 3$ states calculated using the various methods. The full curves are from the present close-coupling (CC) calculation, the dotted curves are from the eikonal impulse distorted wave approximation (EIA) (Rodriguez and Miraglia 1994) and the broken curves are from the one-centre atomic orbital expansion (1C) calculation (Ford *et al* 1994). The overall energy dependence from these calculations are the same except for the EIA calculations for excitation to 3p at low energies where it predicts the cross section rising with decreasing collision energies. This behaviour may be an indication of the failure of the EIA at lower energies. In general, our close-coupling calculation results agree better with the one-centre expansion calculation. The comparisons are shown in figure 3. The open circles are from the close-coupling calculation, and the full circles are from the one-centre expansion calculation. The agreement becomes better at collision energies above 30 keV.

3.2. Propensity rule and magnetic substate distributions

We next examine the population of the magnetic substate distributions for the 3p and 3d states which are excited from the H(2s) initial state. To examine the propensity rule, the

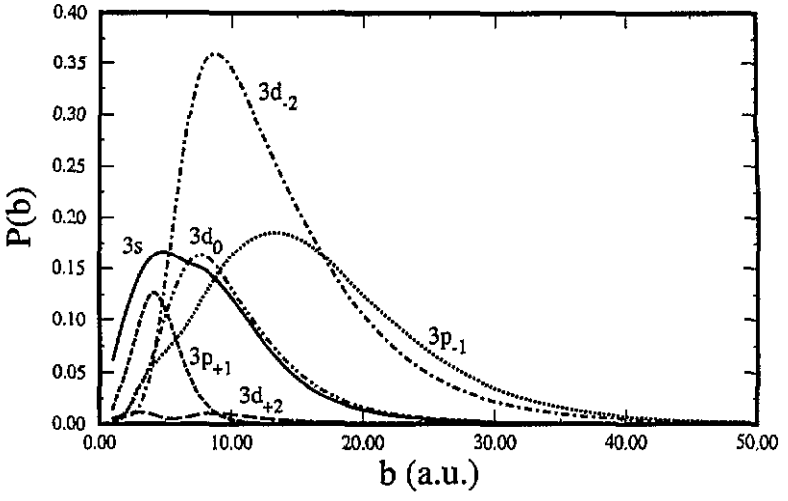

Figure 4. Excitation probability to H($3lm$) in the 'natural' frame, where the quantization axis is taken to be perpendicular to the collision plane at 25 keV impact energy.

magnetic quantum numbers of the excited states are defined with respect to the z'-axis of the 'natural' frame. In this frame, the collision plane is the $x'y'$ plane, the incident beam is along the x' axis, and the particle is scattered into the $+y'$ direction. The quantization axis z' is perpendicular to the scattering plane such that $x'y'z'$ forms a right-handed Cartesian coordinate system. According to the propensity rule for excitation processes (Anderson and Nielsen 1987, Nielsen and Anderson 1987, Lin *et al* 1989), the dominant magnetic substate populated in the collision satisfies the relation

$$\frac{\langle \Delta\varepsilon \rangle a}{v_M} \approx -\Delta m\pi \tag{1}$$

where $\Delta\varepsilon$ is the energy difference between the initial and final states, a is the effective interaction length and v_M is an impact velocity near the maximum of the excitation cross section. This propensity rule was first derived using a distorted wave approximation, but the validity of this approximation is questionable since the collision system is not perturbative and the initial 2s state is degenerate with the 2p states. Let us consider an impact energy of 25 keV ($v = 1$ au). In figure 4 we plot the excitation probability to the $n = 3$ manifold versus the impact parameter b at 25 keV impact energy. Because the initial state is 2s which is symmetric with respect to the collision plane, the m quantum number of final states must satisfy $l + m =$ even in the 'natural' frame. Thus the $3d_{\pm 1}$ and $3p_0$ states must be excluded. The energy difference between $n = 2$ and $n = 3$ is about 0.07 au, and the interaction length is about 40 au as shown in figure 4. With these parameters, one would predict $\Delta m = -1$ which implies that the $3p_{-1}$ substate would be dominantly populated. But as indicated in figure 4, the $3d_{-2}$ substate has the largest probability followed by $3p_{-1}$. An alternative propensity rule has been proposed by Lundsgaard and Lin (1991) as well as by Roncin *et al* (1990) which has been applied only to electron capture processes so far. According to this propensity rule, the dominant magnetic substates that are populated after an electron capture process are those with $m = -l$ for each l for this choice of coordinates. The origin of this propensity rule is attributed to the rotational coupling in ion–atom collisions and has nothing to do with perturbation theory. With respect to the natural frame, the $m = -l$ substates have the same of sense of rotation as the rotation of the internuclear axis, and

these substates have maximal density near the collision plane. This means that when the electron is captured or excited, it not only tends to rotate the same way as the internuclear axis but also moves close to the collision plane.

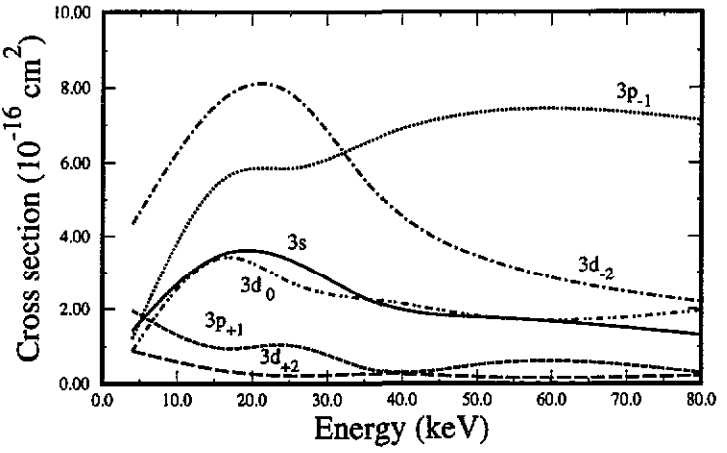

Figure 5. Excitation cross section to H($3lm$) in the 'natural' frame.

In figure 5 we plot the excitation cross sections to different magnetic substates of the $n = 3$ manifold. For the whole energy range covered, it is clear that the $m = -l$ propensity rule applies. Thus we conclude that the same propensity rule holds for both the excitation and the charge transfer processes. This is not surprising in view of the 'origin' of the propensity rule: the rotational coupling causes the electrons near the collision plane to rotate in the same direction as the rotation of the internuclear axis. This mechanism would populate the $m = -l$ substates irrespective of whether it is an excitation or a charge transfer process. We emphasize that this propensity rule applies near the velocity matching region only. It is not applicable to collisions at low velocities.

3.3. Dipole moments

We also calculated the dipole moment, $\langle D_Z \rangle$, of the excited $n = 3$ states at various impact energies. The dipole moment is defined here as

$$\langle D_Z \rangle_{n=3} = 6\sqrt{6} Re \left(\bar{\rho}_{00,10} + \sqrt{\tfrac{1}{2}} \bar{\rho}_{10,20} + \sqrt{\tfrac{3}{2}} \bar{\rho}_{11,21} \right) \Big/ \mathrm{Tr}(\bar{\rho}_{n=3}) \tag{2}$$

where $\bar{\rho}_{lm,l'm'}$ are the density matrix elements written in the the form of the scattering amplitudes, $a_{nlm}(b)$, integrated over the impact parameter b

$$\bar{\rho}_{lm,l'm'} = \int_0^{2\pi} \int_0^{\infty} a_{3lm}(b) a^*_{3l'm'}(b) b \mathrm{d}b. \tag{3}$$

Figure 6 shows $\langle D_Z \rangle$ from the present close-coupling calculation (full curve) and the EIA calculation by Rodriguez and Miraglia (dotted curve). The two calculations agree with each other very well at impact energies above 35 keV, but large differences occur at lower collision energies. The latter may be a further indication that the EIA does not apply to

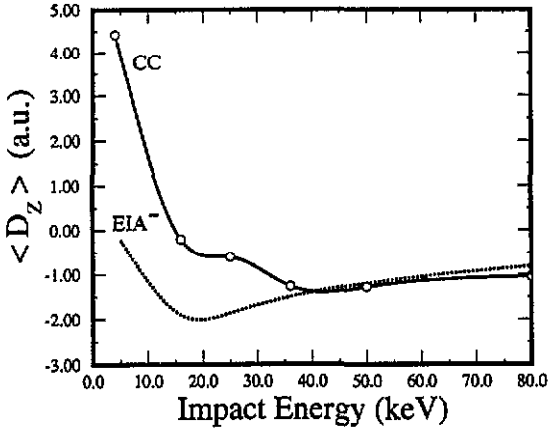

Figure 6. The averaged dipole moment $\langle D_Z \rangle$ of H($n = 3$). Full curve, the close-coupling calculation; dotted curve, the EIA calculation.

the lower energy region where the discrepancies were observed also for the total excitation cross sections (see figure 2).

The calculated average dipole moments are negative at the higher energy points in figure 6. This means that the electron is mostly located ahead of the target after the collision due to the attractive nature of the Coulomb interaction with the projectile, and these results are in agreement with the results obtained for excitation from the ground state, H(1s), by protons (Lin *et al* 1989). At lower collision energies, the dipole moment becomes positive (in the close-coupling calculations). This occurs in the energy region below the peak in the excitation cross section where the propensity rule is no longer valid.

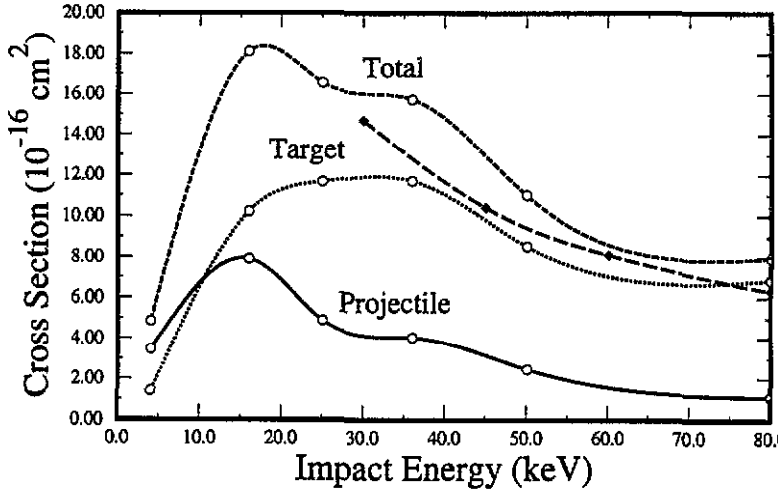

Figure 7. Ionization cross section in p + H(2s) collision. Full curve, total capture to the continuum; dotted curve, direct ionization; broken curve, total ionization, the sum of capture to the continuum and direct ionization; long broken curve, electron removal. Curves with open circles are the current close-coupling calculations and the curve with full diamonds is from Ford *et al* (1994).

3.4. Ionization cross sections

We have calculated the total ionization cross sections. The results are shown in figure 7. We have also indicated the ionization associated with the pseudostates on the target—traditionally called the direct ionization, and that associated with the pseudostates on the projectile—traditionally called capture to the continuum. It is important to note that the difference between the two is somewhat arbitrary since it depends on how the basis functions are constructed in the calculation, particularly on how the high angular momentum basis functions are chosen. At collision energies above 30 keV, electron capture is almost negligible. The electron removal, which includes electron capture and ionization, is essentially the same as electron ionization. As expected, our total ionization cross section agrees fairly well with the total electron removal cross section by Ford *et al.*

We notice that the total ionization cross section peaks where the excitation cross sections to $n = 3$ and $n = 4$ peak, i.e., around 25 keV. At the peak, the projectile velocity is about twice the initial electron orbital velocity on the target. In this energy region, the cross section is large and, as for the excitation processes, pseudostates with large angular momentum are dominantly populated. We note the similarity to excitation and ionization from the ground state of atomic hydrogen. The excitation cross sections from the ground state of atomic hydrogen to the $n = 2$ states and the ionization cross sections peak around 100 keV (Fritsch and Lin 1983), i.e., where the projectile velocity is twice that of the orbital velocity of the initial target electron.

4. Summary and conclusions

We have calculated excitation and ionization cross sections from the metastable H(2s) state by protons over the energy region of 5–80 keV by using a two-centre atomic orbital close-coupling expansion method. A large basis set was needed, including atomic orbitals with large angular momentum quantum numbers, in order to achieve reasonable convergence. We compared our calculations to those from the recent one-centre atomic orbital expansion method of Ford *et al*, and the agreement is rather good. We also compare our results to the eikonal distorted wave approximation of Rodriguez and Miraglia which is a higher energy theory, but the agreement is also satisfactory in the present energy region. We have also examined the propensity rule for populating magnetic substates in excitation processes, and found that the same $m = -l$ magnetic substates are populated as in electron capture processes. We further examined the dipole moments which measure the coherence of the $n = 3$ substates and the ionization cross sections. Since electron capture is a weak process in the energy region covered, the present work is a comprehensive investigation for the collision of protons with atomic hydrogen in its metastable 2s state.

Acknowledgments

This work is supported in part by the US Department of Energy, Office of Energy Research, Office of Basic Energy Sciences, Division of Chemical Sciences and in part by the US–Argentina Cooperative Research Program.

References

Anderson N and Nielsen S E 1987 *Z. Phys.* D **5** 309
Blanco S A, Falcon C A, Reinhold C O, Casaubon J I and Piacentini R D 1987 *J. Phys. B: At. Mol. Phys.* **20** 6295
Blanco S A, Falcon C A, Reinhold C O and Piacentini R D 1986 *J. Phys. B: At. Mol. Phys.* **19** 3945
Campbell E E B, Hülser H, Witte R and Hertel I V 1990 *Z. Phys.* D **16** 21
Dowek D, Houver J C, Pommier J, Richter C, Royer T, Andersen N and Palsdottir B 1990 *Phys. Rev. Lett.* **64** 1713
Dubois A, Nielsen S E and Hansen J P 1993 *J. Phys. B: At. Mol. Opt. Phys.* **26** 705
Esry B D, Chen Z, Lin C D and Piacentini R D 1993 *J. Phys. B: At. Mol. Opt. Phys.* **26** 1579
Ford A L, Reading J F and Hall K A 1994 *J. Phys. B: At. Mol. Opt. Phys.* to be published
Fritsch W and Lin C D 1983 *Phys. Rev.* A **27** 3361
—— 1991 *Phys. Rep.* **202** 1
Lin C D, Shingal R, Jain A and Fritsch W 1989 *Phys. Rev.* A **39** 4455
Lundsgaard M and Lin C D 1992 *J. Phys. B: At. Mol. Opt. Phys.* **25** L429
Nielsen S. E and Anderson N 1987 *Z. Phys.* D **5** 321
Richter C, Andersen N, Brenot J C, Dowek D, Houver J C, Salgado J and Thomsen J W 1993 *J. Phys. B: At. Mol. Opt. Phys.* **26** 723 and references therein
Rodriguez V D and Miraglia J E 1994 to be published
Roncin P, Adjauri M N, Guillemot L, Barat M and Andersen N 1990 *Phys. Rev. Lett.* **66** 3261
Schultz D R, Olson R E, Reinhold C O, Gealy M W, Kerby G W III, Hsu Ying-Yuan and Rudd M E 1991 *J. Phys. B: At. Mol. Opt. Phys.* **24** L599
Shakeshaft R 1978 *Phys. Rev.* A **18** 1930